Earthquake Engineering, Tenth World Conference © 1992 Balkema, Rotterdam. ISBN 90 5410 060 5

Experimental study on deformation capacity of reinforced concrete shear walls after flexural yielding

T. Nakachi, T. Toda & T. Makita
Hazama Corporation, Japan

ABSTRACT: This paper describes the deformation capacity of multistory reinforced concrete shear walls after flexural yielding. Lateral loading tests on five shear walls were conducted. The primary variables were (a) the boundary column concrete confinement i.e. the amount of reinforcing hoop in the boundary columns, (b) the type of concrete confinement in the panels, and, (c) the percentage of steel used in the panels. Compression tests were conducted on square and rectangular sections of columns (which simulated the boundary columns and panels) to investigate the effect of the confining reinforcing. The relationship between the compressive ductility of the boundary columns and panels and the deformation capacity of shear walls was then analyzed.

1 INTRODUCTION

Multistory shear walls installed in high-rise reinforced concrete buildings effectively reduce seismic vibration. In order to improve the seismic performance of such shear walls, it is best that the failure modes of the shear walls are flexural as a flexural mode is the most ductile kind of failure mode. Flexural-type shear walls have a hinging region at the base. The deformation capacity of this region greatly affects the overall deformation capacity of the shear wall. When multistory shear walls are laterally loaded during an earthquake, the boundary columns and panels in the hinging region are subjected to high compressive and shear stress. Reinforcing the boundary columns or panels is therefore effective in improving the deformation capacity of shear walls. This paper examines the relationship between the degree of confinement or reinforcing in the boundary columns and panels and the deformation capacity of the shear wall. Evaluation was based on the results of multistory shear wall lateral loading and compression tests. The column compression tests simulated the boundary columns and panels.

2 LATERAL LOADING TEST OF SHEAR WALLS

2.1 *Test specimen*

Five one-fifth scale shear wall specimens were tested. Each of the specimens represented the shear walls of the lower three stories in a building of approximately thirty stories. The variables included the amount of hoop reinforcing in the boundary columns, the type of confining steel used in the panels, and the percentage of horizontal steel used in the panels. The configurations and dimensions of the specimens are shown in Fig.1. The specimens were 1380mm in height, the panels were 60mm in thickness, and the percentage of vertical steel used in panels was 0.7% of panel. The boundary

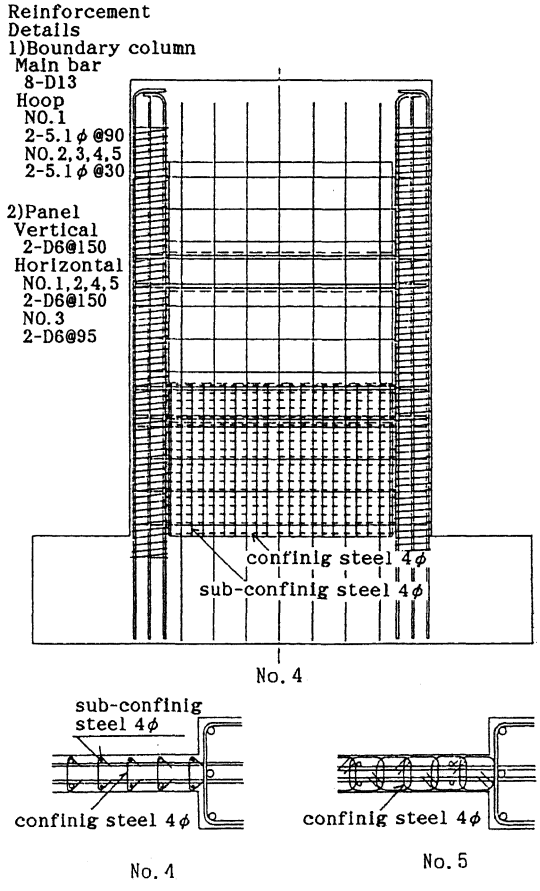

Fig.1 Test Specimens

columns had a (180mm measuring x 180mm) square cross section.

D13 and D6 deformation bars were the main kind of reinforcing bars used in the boundary columns and the panels respectively. The high-strength reinforcing bars 5.1ϕ and 4ϕ were used for the boundary column hoop reinforcing and the panel confining bars respectively.

The boundary column main reinforcing ratio was 3.14% for all the specimens.

The maximum aggregate size was 13mm. The physical properties of the concrete and reinforcing are listed in Table 1 and 2.

Specimen NO.1 was designed to have a law transverse reinforcing ratio of 0.2% while the high transverse reinforcing ratio of NO.2 stood at 0.7%.

Specimen NO.3 was designed to have a high wall horizontal reinforcement ratio of 1.2%. This contrasts with Specimen NO.2's horizontal reinforcement ratio which stood at 0.7%.

Specimens NO.4 and NO.5 were confined at the first story of the panel using tie bar and closed reinforcing.

2.2 *Test procedures*

The loading tests were conducted as shown in Fig.2 and Fig.3. In the lateral loading tests, the specimens were subject to forces from an actuator connected to the reaction wall. A constant axial loading force of 9.8MPa was applied to each boundary column. The added moment was loaded in proportion to the lateral loading in order to keep the shear span ratio (2) at the bottom of the shear wall. Two actuators were vertically connected to the reaction frame to achieve this.

The loading was controlled by the horizontal drift angle at the first story (h:700mm). The loading program is listed in Table 3.

2.3 *Test results*

Fracture process The test results are listed in Table 4. In every test, flexural cracks first appeared at the bottom of the boundary column on the side being stretched. Next, shear cracks appeared at the panel bottom on the side being stretched. Shortly after that, the panel vertical reinforcing and the boundary column main reinforcing

Table 1 Physical Properties of Concrete

specimen	σb (MPa)	Ec ($\times 10^4$MPa)	σt (MPa)
NO.1	37.4	2.95	-
NO.2	38.1	2.55	-
NO.3	39.2	2.95	2.3
NO.4	40.5	2.99	2.4
NO.5	41.0	2.95	2.9
SCT	42.4	3.06	2.8
ECT	46.7	2.89	2.8

σb: compressive strength
Ec: Secant Modulus at σb/3
σt: splitting tensile strength
SCT: compressive test specimen(at start)
ECT: compressive test specimen(at end)

Table 2 Physical Properties of Reinforcing

type of reinforcing	σy (MPa)	σu (MPa)	Es ($\times 10^5$ MPa)	εu (%)
4ϕ (NO.3,4,5)	987.9	1450.5	1.95	5.5
5.1ϕ (NO.1,2)	1388.4	1483.7	2.13	11.4
5.1ϕ (NO.3,4,5)	1334.8	1413.9	2.01	8.7
D6 (NO.1,2)	367.5	508.3	1.79	14.1
D6 (NO.3,4,5)	402.2	521.3	1.83	25.2
D13 (NO.1,2)	378.1	550.0	1.89	18.8
D13 (NO.3,4,5)	362.7	526.3	2.02	19.2

σy: Yield strength
σu: Tensile strength
Es: Young's Modulus
εu: Elongation

Table 3 Loading Program

Cycle	1	2,3	4,5	6,7	8,9	10,11	12	13
R($\times$10 rad.)	1	2	5	7.5	10	15	20	last

R: Drift angle

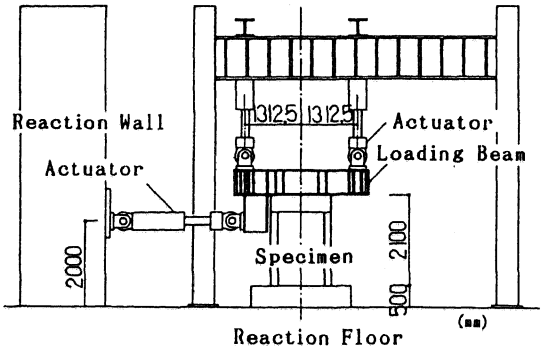

Fig.2 Test Setup

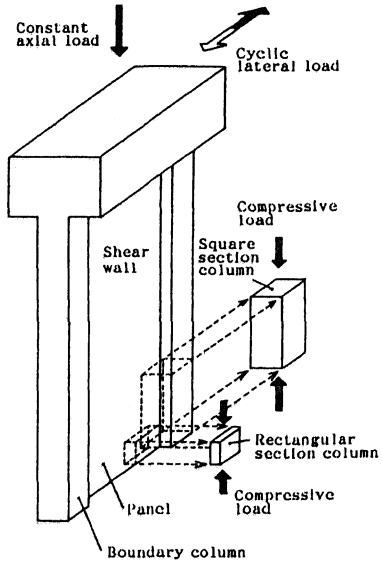

Fig.3 Loading System

yielded. The bottom of the boundary column on the side being compressed also appeared to crumble a little during this time. Eventually, the panel horizontal reinforcing and the beam main reinforcing yielded.

The flexural strength of the shear walls was calculated through fiber model analysis. The equations previously mentioned, matched the experimental results fairly closely.

Load deflection curves Fig.4 shows the load deflection curves. The load of Specimen NO.1 decreased rapidly during the second cycle (15/1000rad.) due to the concrete at the bottom of the boundary column and the panel being crushed. The load of Specimen NO.2 decreased after it had exceeded 15/1000 rad. This was due to the bottom panel slipping and no crumbling occurred. Specimens NO. 3,4 and 5 kept withstood most of the maximum loads until 40/1000rad.. There was little difference between NO.3, 4 or 5. At the final stage, NO.3 crumbled in the compressive region at the bottom of the panel. NO.5 slipped at the bottom of the panel.

Fig.6 shows the load deflection envelope curves. The deformation capacity of Specimen NO.3 (which was designed to have a high wall horizontal reinforcement ratio of 1.2%) increased. The deformation capacity of Specimens NO.4,5 (which were confined at the first story of the panel using tie bar and closed reinforcing) increased.

Crack patterns Fig.5 shows the crack pattern of Specimen NO.3 during the final stages. The test specimens all had similar crack patterns. Shear cracks with a constant angle appeared before 2/1000rad., and after 5/1000rad., cracks appeared in a radial manner with the bottom of the boundary column on the side being compressed being at the center. The number of shorter cracks that appeared at the first story of Specimen NO.5 was greater than that of other specimens.

3 COMPRESSION TESTS

3.1 *Test specimens*

Twenty one specimens (see Fig.7, Table 5) were tested. The variable of the boundary column specimens (C0001 ~ C0703) was the amount of the transverse reinforcing. The variable of the panel specimens (W0001 ~ W0503) was the type of concrete confinement. The specimens were made from the same materials as the specimens used in the shear wall lateral loading tests.

3.2 *Test procedures*

The specimens were subject to monotonic uni-axial compression. Axial strain was measured with transducer (see Fig.8 for measuring length). Strain gauges were attached to both longitudinal and transverse reinforcing.

3.3 *Test results*

Fig.9 shows the relationship between specimens axial

Table 4 Test Results

	NO.1	NO.2	NO.3	NO.4	NO.5
Eo(KN/cm)	2303.0	3518.2	4694.2	3900.4	3900.4
Qfc(KN)	91.1	206.8	187.2	127.4	147.0
Qsc(KN)	164.6	177.4	226.4	177.4	225.4
Qym(KN)	351.8	391.0	381.2	348.9	358.7
Qyb(KN)	397.9	333.2	410.6	400.8	386.1
Qyv(KN)	324.4	364.6	381.2	378.3	384.2
Qyh(KN)	324.4	402.8	407.7	402.8	392.0
maxQexp(KN)	401.8	413.6	415.5	403.8	396.9
maxQcal1(KN)	406.7	406.7	402.8	402.8	403.8
maxQcal2(KN)	392.0	392.0	388.1	388.1	388.1
maxQcal3(KN)	418.5	418.5	401.8	401.8	401.8

Eo: Initial stiffness
Qfc: Flexural cracking load
Qsc: Shear cracking load
Qym: Load at yielding of main reinf.
Qyb: Load at yielding of beam main reinf.
Qyv: Load at yielding of vertical reinf. in panel
Qyh: Load at yielding of horizontal reinf. in panel
maxQexp: Maximum strength(experimental results)
maxQcal1: Maximum strength(calculation 1)
maxQcal2: Maximum strength(calculation 2)
maxQcal3: Maximum strength(calculation 3)

calculation1: (A.I.J. 1990)

$$Qmu=Mu/H \quad Mu=0.9at\cdot\sigma y\cdot D+0.4aw\cdot\sigma wy\cdot D+0.5ND(1-N/(BcDFc))$$

calculation2: (A.I.J. 1990)

$$Mu=at\cdot\sigma y\cdot lw+0.5aw\cdot\sigma wy\cdot lw+0.5N\cdot lw$$

calculation3: (S.Fuji 1973)
fiber model analysis

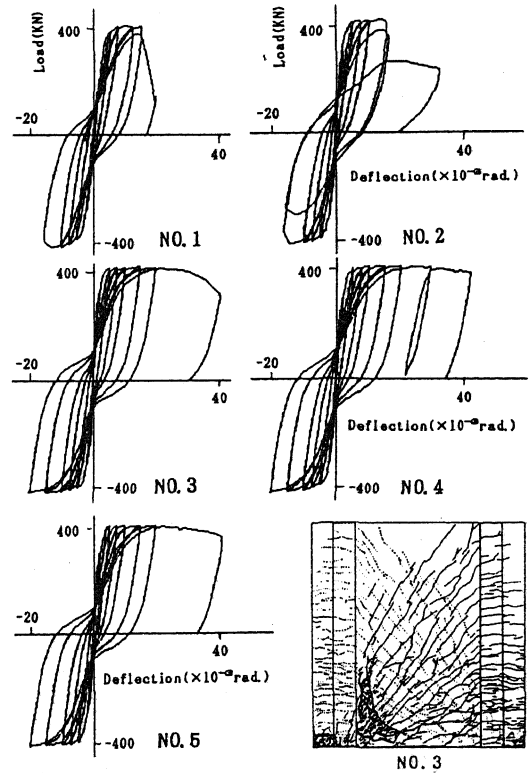

Fig.4 Load Deflection Curves

NO. 3

Fig.5 Crack Pattern

compression stress and axial strain. The maximum and post-failure stresses of Specimen C0701 (Pw=0.7%) which simulated the boundary columns of shear wall specimens NO.2,3,4 and 5, were much higher than the stresses of Specimen C0203 (Pw=0.2%) which simulated the boundary columns of Specimen NO.1.

Specimen W0502 which was confined with closed reinforcing and which simulated the panel of Specimen NO.5, showed the highest maximum and post-failure stresses. The second highest was Specimen W0402 which was confined with tie bars and simulated the panel of Specimen NO.4.

Fig.10 shows the relationship between the strain of the transverse reinforcing or confining reinforcing and the axial strain of the specimens.

The strain of Specimen C0701's transverse reinforcing increased as the axial strain increased, indicating an increase in confining stress. Although the transverse reinforcing strain increment rate decreased after the point maximum axial stress was ruled, strain continued to increase within measurable range.

On the panel specimens, Specimen W0501,which simulated the panel of Specimen NO.5, behaved in a similar manner to boundary column specimen C0701. Specimen W0402, which simulated the panel of Specimen NO.4, showed decrease in confining reinforcing strain for axial strain exceeding a certain level.

4 ANALYSIS TEST RESULTS

4.1 *Strain distribution in boundary columns*

Fig.11 shows the strain distribution in the boundary column of the shear wall specimen NO.1. The strain was measured using the transducer located 60mm from the edge of the shear wall. The tensile hinging region expanded in a vertical direction as the drift angle increased.

The compressive hinging region was concentrated around the bottom of the boundary columns. Judging from this, it is possible to conclude that confining concrete with lateral reinforcing in the region helps deformation capacity in multistory shear walls.

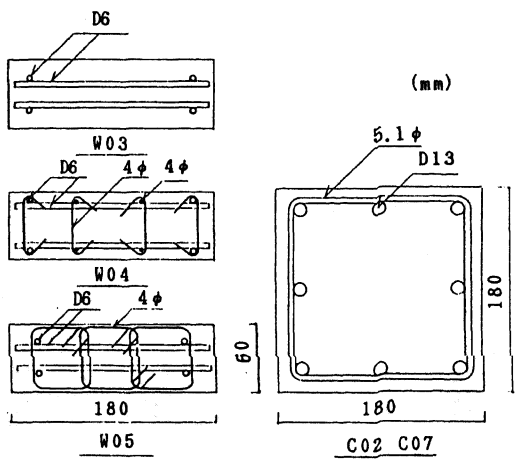

Fig.7 Test Specimens

4.2 *Boundary column base compressive strain*

Fig.12 shows the relationship between the drift angle and compressive strain at the bottom of boundary

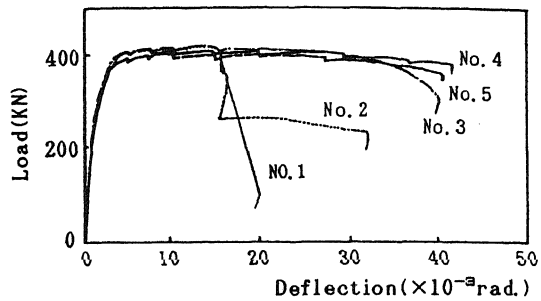

Fig.6 Load Deflection Envelope Curves

Table 5 Test Specimens

Specimen	Max. Load (KN)	Strain at Max. Load(%)
C0001	1228.9	0.31
C0002	1181.9	0.40
C0003	1318.1	0.26
C0201	1384.7	0.24
C0202	1458.2	0.31
C0203	1457.3	0.37
C0701	1650.3	0.71
C0702	1635.6	0.43
C0703	1679.7	0.68
W0001	338.1	0.99
W0002	408.7	0.74
W0003	374.4	0.70
W0301	383.2	0.68
W0302	383.2	0.66
W0303	427.3	0.95
W0401	396.9	0.59
W0402	454.7	0.98
W0403	505.7	1.04
W0501	532.1	1.38
W0502	545.9	1.41
W0503	660.5	2.38

boundary column specimen C0201 — Pw=0.2%

panel specimen W0301 — simulating specimen NO.3

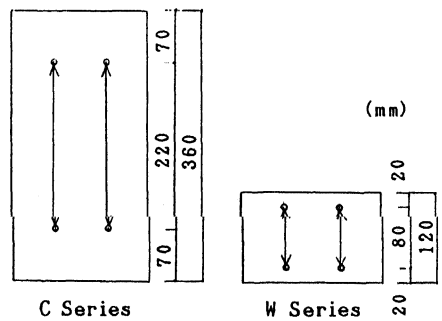

Fig.8 Measuring System

columns. The strain was measured with a transducer located 60mm from the edge of the shear wall. The measuring length was 180mm. Compressive strain increased in proportion to the drift angle. The compressive strain for each of the five shear wall specimens was approximately the same for angles up to 10/1000rad.. One exceeded, the strain of Specimen NO.1 increased rapidly.

The average axial strain at the point of maximum axial compressive stress for the boundary column specimens C0201,C0202 and C0203 (Pw=0.2%)(which simulated the boundary column of Specimen NO.1), was 0.307% (see Table 5). The compressive strain at the bottom of Specimen NO.1's boundary columns, however, was approximately 0.5% and 1.0% for the drift angles of 10/1000rad. and 15/1000rad. respectively (see Fig.12). The axial compressive stress of Specimen C0203 also decreased a great deal at an axial strain of 0.5% and 1.0% (see Fig.9(a)). From these results one may conclude that the compression tests results reflect the rapid decrease in Specimen NO.1's load what is caused by the boundary column reaching crumbling point at 15/1000 rad.

Until reaching an axial strain of 6.0%, Specimen C0701 (Pw=0.7%) maintained its axial stress for a longer period than Specimen C0203's (Pw=0.2%) maximum stress. These results correspond to the non-crumbling of the boundary columns of the shear wall specimens NO.2,3,4 and 5.

4.3 *Strain distribution of confining reinforcing at panel along span*

The load of shear wall specimen NO.2 decreased after 15/1000rad. due to destruction of the panel, even though no crumbling occurred at the base of the boundary columns. Destruction of the panel was thought to be due to crumbling through compressive stress or through the failure of the shear-resisting mechanism.

The confining reinforcing in the panels of Specimens NO.4 and NO.5 was arranged to improve the panel's compressive ductility. The effects of confinement are shown in Fig.9(b), 10(b) and 10(c). An increase in confining reinforcing strain reflects an increase in confining stress (see Fig.10(a) and 10(b)). It can therefore be concluded that the compressive ductility of the panel specimens was improved (see Fig.9(b)).

Fig.13, 14 shows the confining reinforcing strain distribution of the span at the bottom of the panel of shear wall specimens NO.4 and NO.5 respectively.

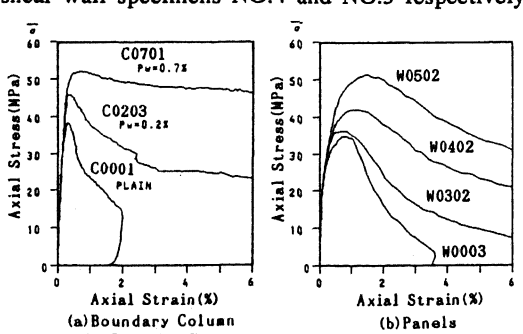

Fig.9 Axial Stress versus Axial Strain

Distribution is shown at a height of 125mm.

Strain increased near the compressive boundary column with the increase in drift angle in both NO.4 and NO.5 specimens. Strain in Specimen NO.5 was larger than that in Specimen NO.4 for the entire length of the span. As the amount of confining reinforcing in Specimen NO.4 and NO.5 was approximately the same, the confining stress of Specimen NO.5 was considered to be higher than that of NO.4. Specimen NO.5's range of strain increase was greater than that of NO.4. *Specimen NO.4's concentrated strain increase range* was also near the compressive boundary column. Judging from the strain distribution patterns, confining reinforcing is regarded to be more effective when used to confine concrete near the boundary columns. It is therefore desirable that confining reinforcing be

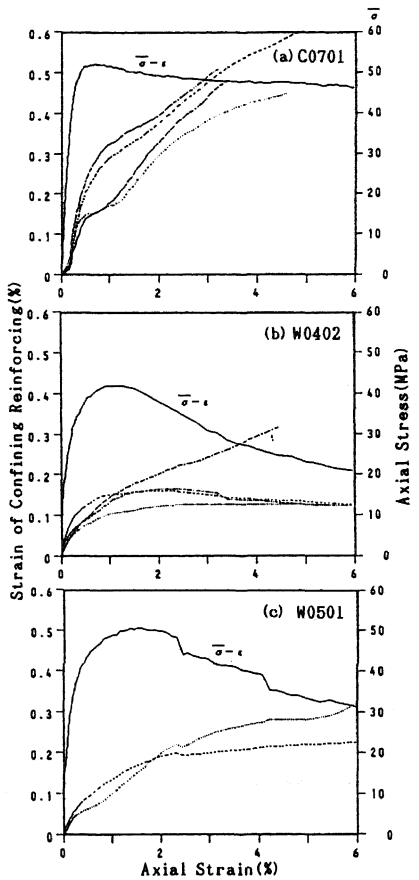

Fig.10 Strain of Confining Reinforcing versus Axial Strain

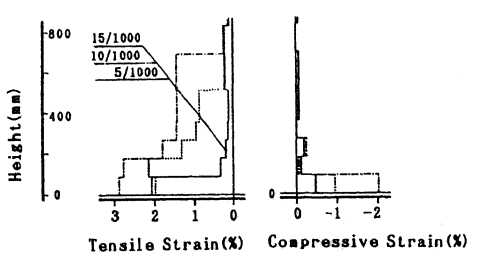

Fig.11 Strain Distribution in Boundary Column

employed as a means of improving the deformation capacity of multistory shear walls.

Fig.15 shows Specimen NO.5's confining reinforcing strain and lateral load hysteresis loops for the panel base (height 125mm) near the boundary column (inside of column by 60mm).

In this figure, the measuring point was located in the compressive region as lateral loading was positive. The concrete in the panel was therefore considered to be confined by confining reinforcing during concrete compression.

As a result, concrete confinement through confining reinforcing in the panel helped to improve the compressive ductility of the panel, and improve the deformation capacity of the multistory shear wall.

4.4 *The effect of the horizontal reinforcing in panels*

Fig.16 shows the relationship between the drift angle and the horizontal reinforcing strain for the first story of the shear wall specimens NO.2 and NO.3 panels at medium height. Strain in Specimen NO.2 was larger than that in Specimen NO.3 for the measuring points in the mid span and near the boundary column. In spite of the yielding of Specimen NO.2's reinforcing at approximately 15/1000 rad., the reinforcing of Specimen NO.3 did not yield until 30/1000 rad. These drift angles correspond to the drift angles at which the specimen load decreased markedly.

From these results one may conclude that the deformation capacity of a shear wall may be increased by increasing the amount of horizontal reinforcing in the panel. More horizontal reinforcing reduces the amount of stress on the reinforcing which results in a shear wall with a greater ability to resist shear forces.

5 CONCLUSIONS

1. The concrete confinement of the boundary columns were observed to illustrated by the compressive crumbling of the boundary columns or panels.
2. The compressive hinging region was concentrated at the base of the boundary columns. The compressive strain of concrete at the end was observed to be nearly in proportion to the drift angle.
3. The deformation capacity of the shear wall increased as the ratio of the horizontal reinforcing in the panels increased.
4. The confinement of the concrete using the confining reinforcing in the panels had a significant effect on the deformation capacity.
5. The flexural strength of the shear walls calculated through fiber model analysis and the equations previously mentioned, matched the experimental results fairly closely.

REFRENCE

1) AIJ 1990. Ultimate strength and deformation capacity of buildings in seismic design(in Japanese). *AIJ* : Japan.
2) Fujii,S., H. Aoyama & H. Umemura. Load-curvature relation of rein forced concrete sections calculated using material properties(in Japanese). *Summaries of technicalpapers of annual meeting architectural institute of Japan* :1261-1262

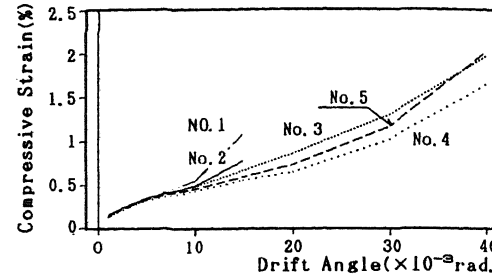

Fig.12 Drift angle versus Compressive Strain at Base of Boundary Columns

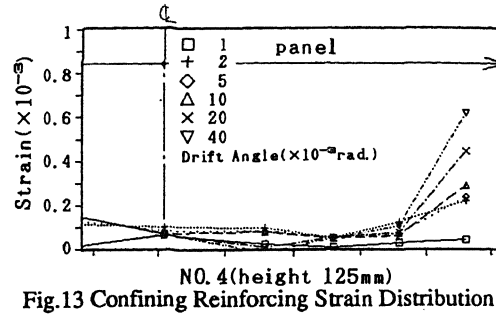

Fig.13 Confining Reinforcing Strain Distribution

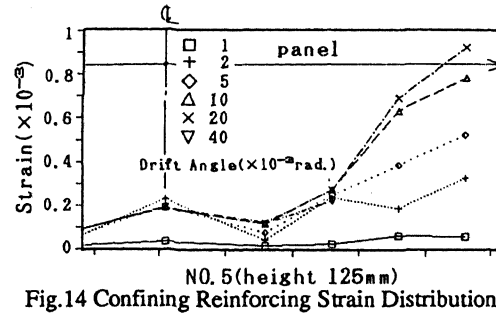

Fig.14 Confining Reinforcing Strain Distribution

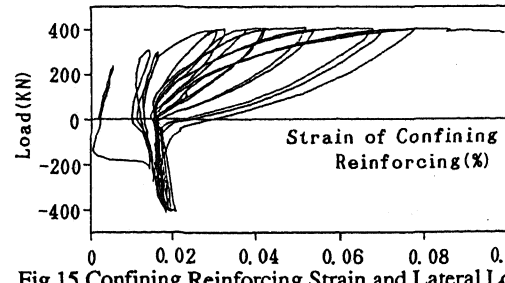

Fig.15 Confining Reinforcing Strain and Lateral Load Hysteresis Loop

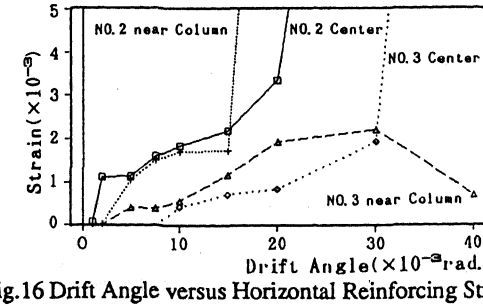

Fig.16 Drift Angle versus Horizontal Reinforcing Strain